Geomorphology 151–152 (2012) 13–26

Contents lists available at SciVerse ScienceDirect

Geomorphology

journal homepage: www.elsevier.com/locate/geomorph

Extending generalized Horton laws to test embedding algorithms for topologic river networks

Ricardo Mantilla [a,*], Vijay K. Gupta [b], Brent M. Troutman [c]

[a] IIHR-Hydroscience & Engineering, The University of Iowa, Iowa City, IA 52242, USA
[b] Department of Civil and Environmental Engineering, Cooperative Institute for Research in Environmental Sciences, University of Colorado, Boulder, CO 80309, USA
[c] U.S. Geological Survey, Denver Federal Center, Lakewood, CO 80225, USA

ARTICLE INFO

Article history:
Received 21 April 2011
Received in revised form 29 December 2011
Accepted 4 January 2012
Available online 18 January 2012

Keywords:
River networks
Embedding algorithms
Random self-similar networks
Self similar trees
Horton laws

ABSTRACT

River networks in the landscape can be described as topologic rooted trees embedded in a three-dimensional surface. We examine the problem of embedding topologic binary rooted trees (BRTs) by investigating two space-filling embedding procedures: Top-Down, previously developed in the context of random self-similar networks (RSNs), and Bottom-Up, a new procedure developed here. We extend the concept of generalized Horton laws to interior sub catchments and create a new set of scaling laws that are used to test the embedding algorithms. We compare the two embedding strategies with respect to the scaling properties of the distribution of accumulated areas A_ω and network magnitude M_ω for complete order streams ω. The Bottom-Up procedure preserves the equality of distributions $A_\omega/E[A_\omega] =^d M_\omega/E[M_\omega]$; a feature observed in real basins. The Top-Down embedded networks fail to preserve this equality because of strong correlations of tile areas in the final tessellation. We conclude that the presence or absence of this equality is a useful test to diagnose river network models that describe the topology/geometry of natural drainage systems. We present some examples of applying the embedding algorithms to self similar trees (SSTs) and to RSNs. Finally, a technique is presented to map the resulting tiled region into a three-dimensional surface that corresponds to a landscape drained by the chosen network. Our results are a significant first step toward the goal of creating realistic embedded topologic trees, which are also required for the study of peak flow scaling in river networks in the presence of spatially variable rainfall and flood-generating processes.

© 2012 Elsevier B.V. All rights reserved.

1. Introduction

The study of river network topology is an active area of research in geomorphology (Meakin et al., 1991; Maritan et al., 1996; Dodds and Rothman, 2000; Molnar, 2005). Several mathematical models have been introduced in the literature to describe, using simple principles, the complex network topology of river networks (Tokunaga, 1966; Scheidegger, 1967; Shreve, 1967; Veitzer and Gupta, 2000). These topologic models have helped put their mathematical foundations on a firm footing, and many of them have been successful in explaining major geomorphic features observed in natural river networks.

Topologic river network models, by definition, only describe how nodes of the network are connected with each other. These models do not provide a description of the spatial embedding of the topology in the three-dimensional landscape of a river basin. As a result, they are unsuitable to study the interaction between spatially correlated rainfall and runoff generation processes and its impact on the transport of flows through a river network. Some network models, such as optimal channel networks (Rigon et al., 1993; Maritan et al., 1996; Rinaldo et al., 2006), Gibbsian networks (Troutman and Karlinger, 1994, 1998), and networks generated by random walks (Leopold and Langbein, 1962; Meakin et al., 1991) include explicitly the spatial geometry of networks by embedding them on a two-dimensional lattice. However, two disadvantages of lattice models relative to topologic models are, first, that generation of lattice models is typically more computationally demanding and, second, that it is more difficult to obtain analytic results for lattice models.

Self-similar river network models play a fundamental role in understanding observed scaling in the magnitudes of peak flows (Gupta et al., 2010). For example, Gupta et al. (1996), Menabde and Sivapalan (2001), and Troutman and Over (2001) considered idealized self-similar networks embedded in a two-dimensional space to understand how the interaction between multifractal rainfall and self-similar river networks determines the magnitude and scaling characteristics of peak flows. Gupta et al. (1996) assumed that rainfall follows spatially correlated beta random cascade that is deposited on a Peano channel network. Likewise, Menabde and Sivapalan (2001) assumed that rainfall follows a log-normal cascade on a Mandelbrot–Viscek network. Troutman and Over (2001) made more general assumptions regarding spatial variability of rainfall and self-similar

* Corresponding author.
E-mail address: ricardo-mantilla@uiowa.edu (R. Mantilla).

0169-555X/$ – see front matter © 2012 Elsevier B.V. All rights reserved.
doi:10.1016/j.geomorph.2012.01.002

network structure to study scaling in peak flows. In all these studies, however, the spatial cascade structure of rainfall was assumed to be aligned with the topology of the network. Mantilla (2007) conducted simulation of scaling in peak flows on RSNs. In order to generalize this approach to spatially correlated rainfall embedding realistic[1] topological networks in a three-dimensional space is necessary.

The embedding process is schematically illustrated in Fig. 1 for a very simple network topology. We begin with, first, a network for which it is assumed that only the connectivity structure (a topologic tree) is known (Fig. 1a) and, second, a two-dimensional region with a fixed shape (Fig. 1b) into which the network will be embedded. The goal is to develop an algorithm, which yields the embedded network, as shown in Fig. 1c. The embedding process, as defined in this paper, must therefore fulfill two minimal requirements: (i) it must be space filling, which means that every point in the given region has to be assigned to, or drain into, a unique link of the binary rooted tree (BRT); the process is known as tiling, and (ii) the topologic structure of the network needs to be preserved.

These two minimal requirements of the embedding process do not uniquely define an algorithm for obtaining the embedded network, so clearly any proposed procedure needs to be further tailored so as to preserve, to the extent possible, important geometrical properties of real drainage basins. Examination of Fig. 1c makes clear that the distribution of the size of areas assigned to the individual links, and the resulting size of accumulated areas of sub basins is a fundamental characteristic of embedded networks. It is the focus here. A key contribution of this paper is to apply generalized Horton's laws (Peckham and Gupta, 1999; Veitzer and Gupta, 2000; Troutman, 2005) to obtain a sensitive measure of how well the area distribution of embedded networks conforms with behavior observed in real networks.

Generalized Horton's laws are based on the idea of statistical self-similarity (SSS) of the distribution of basin variables defined for streams of different Strahler orders (Strahler, 1957). Strahler ordering of streams is determined by the following rules: first-order streams are those with no upstream inflows and the stream immediately downstream from the junction of two streams of order ω_1 and ω_2 is ω_1+1 if $\omega_1=\omega_2$ and the maximum between ω_1 and ω_2 if $\omega_1\neq\omega_2$. The two basin variables of interest here are drainage area, A, and network magnitude, M, defined as the number of first-order streams in the network. A comparison of the statistical distribution of these two variables provides a test of embedding algorithms.

In Section 2 we provide some background on the problem of embedding BRTs and also present data from real networks. In Section 3, the concept of basin decomposition into hillslopes is used to introduce an extension of Horton's laws (Horton, 1945; Strahler, 1957). It is used to test the properties of the tessellations generated by our embedding strategies. In Section 4 we present two embedding strategies. First, in Section 4.1 we present the embedding procedure that Veitzer (1999) developed that we call the top-down embedding (TDE) algorithm. We explain the deficiencies of this algorithm with respect to the generalized Horton's laws. In Section 4.2 the bottom-up embedding (BUE) algorithm is described, and advantages of using this approach are explained. Some examples of the BUE are presented using self similar trees (SSTs) and RSNs. In Section 5 we develop a method to generate three-dimensional landscapes using the tiled region obtained by the BUE. Finally, in Section 6 our conclusions are presented and areas of future research are highlighted.

[1] The term *realistic* refers to topological networks that emulate scaling features observed in natural river networks, such as Horton laws, Hack's law, the tail of cumulative areas, properties of the width function, etc. (see Rodríguez-Iturbe and Rinaldo, 1997, Chapter 1)

2. The RSN river network model and the embedding problem

Topologic network models have a long history in hydrology. The earliest topologic model was introduced by Shreve (1966), and it is known as the random topology model. The model postulates that all topologies of a given magnitude M are equally likely to be observed. After years of intense research, Shreve's model has been proven unsuccessful in predicting many features observed in real river networks such as Hack's law (Mesa and Gupta, 1987) and deviations of Horton ratios from the predicted values. Peckham (1995) studied mean self-similar topologic rooted trees known as Tokunaga trees (Tokunaga, 1966). This deterministic topologic model predicts several topologic features in river basins, including observed Horton ratios that the random model does not (Dodds and Rothman, 2000). McConnell and Gupta (2008) put the results of Tokunaga trees on a firm mathematical footing. However, Tokunaga's model is mean self-similar by definition, and it does not address random variability in the topology and geometry of river networks that is widely observed in nature.

Veitzer and Gupta (2000) introduced a new class of infinite trees known as random self-similar networks (RSNs). This model is of particular relevance to the embedding problem addressed in this paper for three reasons. First, the model produces topologic networks that have been shown to be realistic in many of their features (Veitzer et al., 2003; Troutman, 2005; Mantilla et al., 2010). This is important because if one expects an embedded network to be realistic, the topologic network with which one begins must itself be realistic, so initiating the embedding process with an RSN-generated network is one reasonable way to proceed. Second, the model is based on an iterative replacement process, which readily lends itself to development of embedding algorithms using "generators," which are the building blocks of the iterative process. We shall use generators as the basis of our embedding algorithm, as was done in the work by Veitzer (1999). Third, it is easy to show that the model provides a method to decompose *any* binary tree into a unique sequence of elementary generators, which leads to the original network through the iterative replacement process. This fact makes possible to embed any binary tree using the algorithm, including those obtained by topologic models other than the RSN model.

Random self-similar networks are constructed by replacing, in an iterative fashion, all the links of a network by randomly sampled generators (Veitzer and Gupta, 2000). A generator is defined as the simplest branching pattern (or patterns) selected to generate a more complex branching network using a recursive replacement algorithm. The process of generating a complex branching network, i.e., river network connecting topology, is initiated with a network that consists of a single link that is replaced with a randomly sampled generator. Then the links in the resulting network are all replaced with randomly sampled generators, and so on. Consequently, each step of the iteration process makes the branching structure of the network become more complex. Each link replacement in the iterative process is done in a manner that depends on whether the link to be replaced is "interior" or "exterior," where exterior links are defined as those with no upstream connecting links. Interior links are replaced by generators from one population, known as interior generators, and exterior links are likewise replaced by exterior generators constituting a different population. Construction of RSNs thus requires specification of two probability distributions governing the random sampling of the different generator types, and all sampled generators are assumed to be mutually independent. Fig. 2a illustrates the two populations of generators to be used in this paper, and Fig. 2b illustrates two iterations of the replacement process. Note that interior and exterior generators in this figure are indexed by the number of interior nodes.

The process of reversing this iterative replacement procedure and thereby recovering the unique set of generators from any complex binary network is discussed in detail by Troutman (2005) and Mantilla

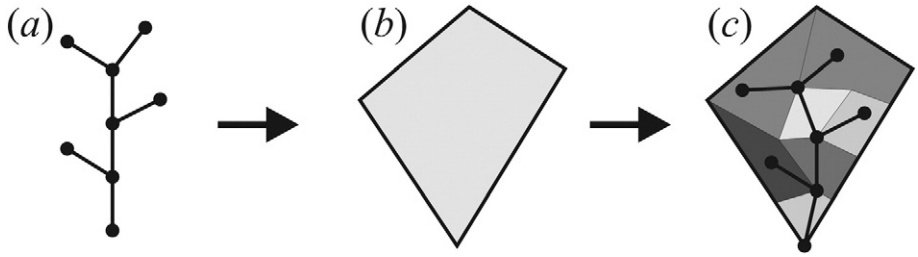

Fig. 1. (*a*) Topologic tree to be embedded. (*b*) Finite two-dimensional region. (*c*) Tiled region.

et al. (2010). In the latter work, this decomposition process was applied to 30 actual drainage basins across the continental United States. They demonstrated that the number of interior nodes for generators in actual networks is well modeled by a geometric probability distribution with parameters that are different for interior and exterior generators. The property of scale invariance was also found to hold for the generators in 26 of the 30 basins in the study. We shall see in the following section that scale invariance forms the basis of our test for embedding algorithms.

3. Extending Horton laws

In this section we will establish a new set of scaling laws for river basins that will allow us to test, in a precise manner, the features of tessellations created by embedding algorithms. The new scaling laws are an extension of the generalized Horton laws based on statistical self-similarity by Peckham and Gupta (1999) involving two fundamental variables: drainage area and network magnitude. Magnitude, a topologic property of networks, is defined as the number of source streams; but drainage area depends on how the network is embedded in space. We shall demonstrate in this section that studying the connection between these two variables via scale invariance allows us to test embedding algorithms.

The extension of Horton laws proposed here is inspired by recent theoretical results by Tokunaga (2003) regarding scaling properties of internal sub basins of Tokunaga trees (Tokunaga, 1966) and other deterministic networks such as the Peano network or the Mandelbrot–Viscek tree. In addition, Troutman (2005) has demonstrated the existence of similar scaling properties for RSN topologies. These results motivate further investigation on natural river networks and the establishment of corresponding scaling laws.

Mantilla and Gupta (2005) developed an algorithm to decompose a basin into hillslopes. This algorithm has enabled us to study the geometric properties of landscape tessellation imposed by the existence of river network. Fig. 3 shows the result of decomposing the 2.13-km^2 order-3 Quartz Hill basin in central New Mexico into hillslopes (Fig. 3a). This decomposition identifies the link–hillslope pairs, as they exist on the landscape. The river network (Fig. 3b) and the set of hillslopes (Fig. 3c) have been superimposed on aerial photography of the area provided via Google Earth ™. The decomposition has also been overlaid on a three dimensional view of the terrain (Fig. 3d) to highlight the meaning of a *level-0* decomposition of the landscape. We distinguish exterior hillslope areas from interior hillslope areas and use the notation $a^{(E)}$ and $a^{(I)}$, respectively, to denote these areas. They are random variables with distinct probability distributions.

The new scaling laws that we will establish are most easily understood when expressed in terms of the *pruned network*. Pruning the network is the process of removing all the order-1 streams from the original network. We will refer to the pruned network as a pseudo-network, composed of pseudo-links. This pseudo-network can be used to decompose a basin into pseudo-hillslopes. The pruning process can be applied iteratively to the pseudo-network to obtain the tessellation corresponding to different pruning levels. Fig. 4 shows the sequence of tessellations obtained by iteratively pruning the network of the order-3 Quartz Hill basin.

We identify an important connection between pruning and Strahler ordering of the network (Strahler, 1957). We see that pruning the network once removes all order-1 streams, pruning the network twice removes all order-2 and lower streams, and in general pruning the network i times removes all order-i and lower streams. Thus, the index i for a given decomposition level corresponds to the order $\omega = i$

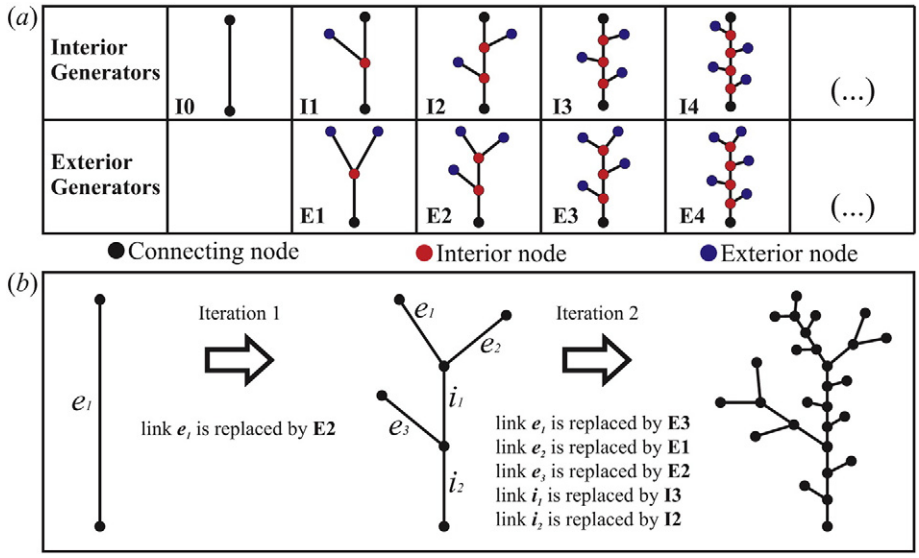

Fig. 2. (*a*) Path-based generators. (*b*) Iterative replacement process to create RSNs.

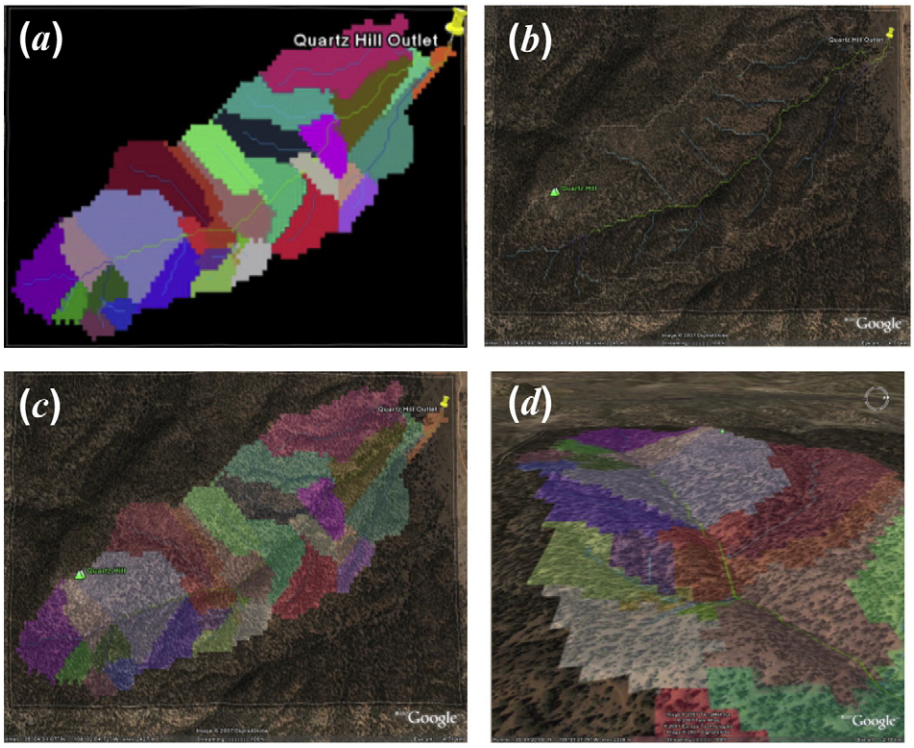

Fig. 3. (*a*) The 2.13-km^2 order-3 Quartz Hill basin in central New Mexico decomposed into hillslopes using the algorithm developed by Mantilla and Gupta (2005). (*b*) River network superimposed on aerial photography of the area provided via Google Earth™, (*c*) transparency of the hillslope units shown on panel (*a*) superimposed over the same aerial image, and (*d*) a three-dimensional view showing the curvature of the landscape adjacent to river network links illustrating convex terrain on hillslopes and concave terrain in channelized terrain.

and lower order streams are pruned away. In other words, a level-0 decomposition corresponds to no pruning, a level-1 decomposition corresponds to removing order-1 streams, a level-2 decomposition corresponds to removing order-2 and order-1 streams, and so on. Therefore, the area of pseudo-hillslopes associated with exterior pseudo-links for a level-i decomposition corresponds exactly to the upstream area of complete order $\omega = i+1$ streams in the original network.

We now proceed to extend the generalized Horton law of drainage areas (Peckham and Gupta, 1999) to obtain a sensitive test for embedding algorithms. If A_ω denotes drainage area of an order ω basin, the classical form of the Horton Law of drainage areas states that the ratio $E[A_{\omega+1}]/E[A_\omega] = R_A$, where $E[\,]$ denotes expectation, is independent of ω and R_A is the Horton ratio of upstream areas (Schumm, 1956). Peckham and Gupta (1999) showed that the upstream areas of complete order streams exhibit statistical simple scaling (SSS). This property was used to generalize Horton law for areas by asserting that

$$A_{\omega+1} \overset{d}{=} R_A A_\omega \tag{1}$$

where $\overset{d}{=}$ means equality of distributions. We see that the generalized Horton's Law for areas describes statistical scaling of exterior pseudo-hillslopes for different pruning levels. Our multi level tessellation technique allows us to extend the concept of generalized Horton laws by investigating the statistical scaling features of interior pseudo-hillslopes. We call this analysis *extended generalized Horton laws* of network composition that apply to $A_\omega^{(E)}$ and $A_\omega^{(I)}$ representing the area of exterior and interior pseudo-hillslopes, respectively, for the pruning level $\omega - 1$. The extended generalized Horton laws are expressed by the relations

$$A_{\omega+1}^{(E)} \overset{d}{=} R_A A_\omega^{(E)} \quad \text{and} \quad A_{\omega+1}^{(I)} \overset{d}{=} R_A A_\omega^{(I)} \tag{2}$$

where $R_A = E[A_{\omega+1}^{(E)}]/E[A_\omega^{(E)}] = E[A_{\omega+1}^{(I)}]/E[A_\omega^{(I)}]$ is a constant independent of ω and the pseudo-hillslope type and $A_\omega^{(E)} \overset{d}{\neq} A_\omega^{(I)}$.

In order to illustrate the extended Horton laws we perform the statistical analysis defined above on two order 8 basins in the US: (i) the 5177-km^2 Walnut Creek River basin in southeastern Kansas and (ii) the 4908-km^2 North Fork Kentucky River basin in northern

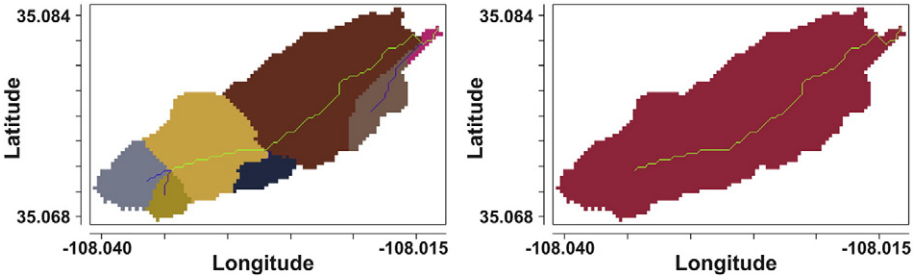

Fig. 4. Decomposition of the basin into pseudo-hillslopes using the pseudo-network obtained by consecutive pruning levels of network.

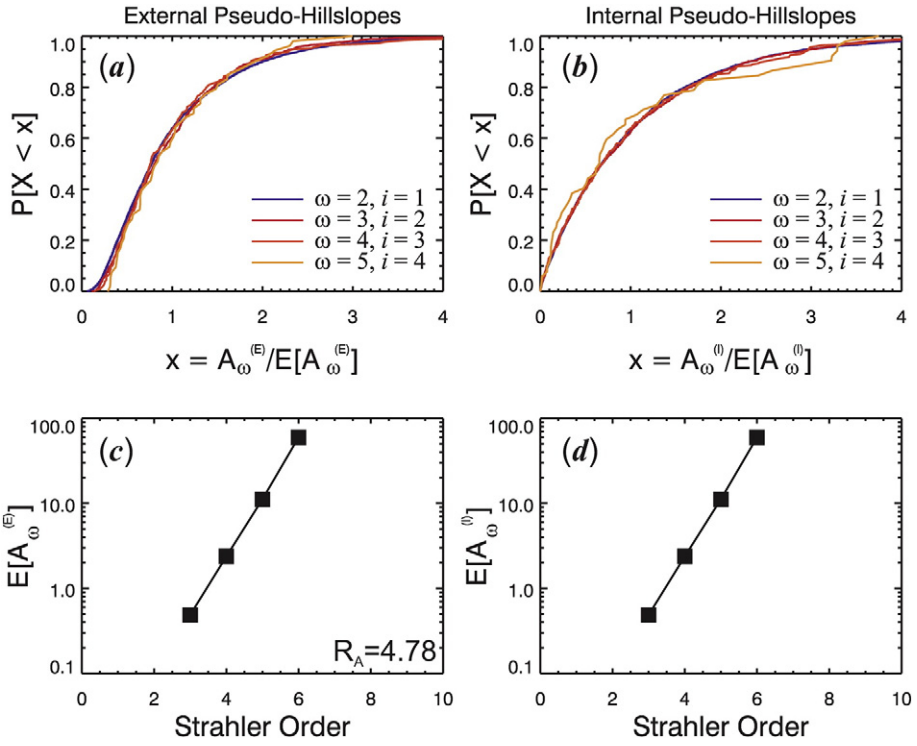

Fig. 5. Extended Generalized Horton laws analysis of areas for the Walnut Creek River basin in southeastern Kansas. Plots (*c*) and (*d*) show mean pseudo-hillsope area (on a logarithmic scale) as a function of Strahler order; R_A is computed by exponentiating the slope of the linear relation. Figs. (*a*) and (*b*) show scaled by the mean pseudo-hillslope area distributions for different orders; collapse of the distributions onto a single curve illustrates the SSS property.

Kentucky. Note that by definition $A_\omega^{(E)} \equiv A_\omega$. Figs. 5 and 6 show the results of this analysis for these two basins.

We see in Figs. 5 and 6 that the scaling observed in previous works for exterior pseudo-hillslopes also holds for interior pseudo-hillslopes. First, plots of mean pseudo-hillslope area on a logarithmically transformed scale versus order are linear for both types, interior and exterior. Also, the slopes are the same for both linear relations. It means that the Horton ratio R_A is the same for both types. The estimated values of R_A are 4.78 and 4.74 for the Walnut River network and the Kentucky River network, respectively. Finally,

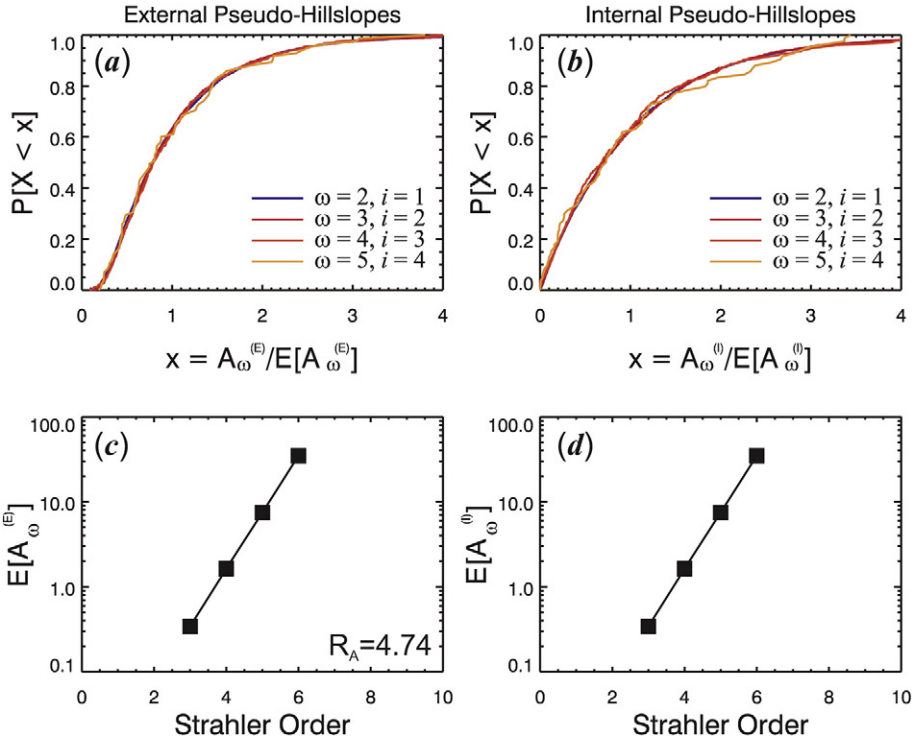

Fig. 6. Extended Generalized Horton laws analysis of areas for the Kentucky River basin in northern Kentucky.

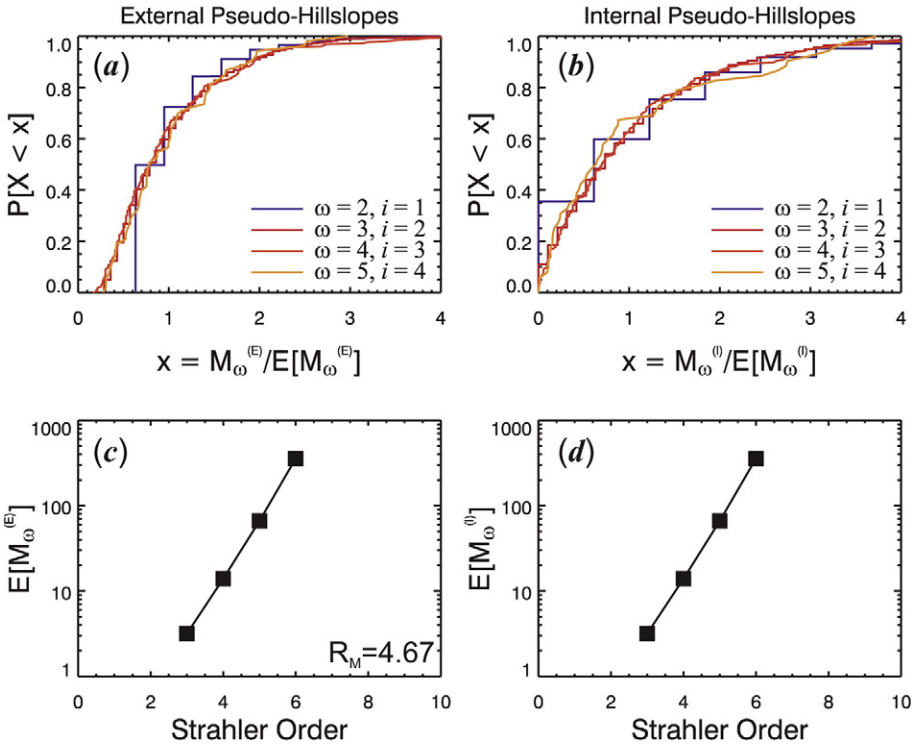

Fig. 7. Extended Generalized Horton laws analysis of pseudo-magnitudes for the Walnut Creek River basin in southeastern Kansas.

pseudo-hillslope areas scaled by their respective means have a distribution independent of order, and the distributions are different for interior and exterior pseudo-hillslope areas.

In a similar fashion to areas, the concept of network magnitude introduced by Shreve (1967) can be extended. Define pseudo-magnitude as the total number of exterior links on the unpruned network contained inside a pseudo-hillslope. As with pseudo-hillslope areas, the pseudo-magnitude of exterior pseudo-hillslopes corresponds exactly to the original concept of magnitude (Shreve, 1967). We denote $M_\omega^{(E)}$ and $M_\omega^{(I)}$ the pseudo-magnitudes of exterior and interior pseudo-hillslopes for the pruning level $\omega-1$. Figs. 7 and 8 show the results of this analysis for the two basins under consideration. Here the estimated values of R_M are 4.67 and 4.62 for the Walnut River network and the Kentucky River network, respectively.

Our analysis shows that

$$M_{\omega+1}^{(E)} \overset{d}{=} R_M M_\omega^{(E)} \quad \text{and} \quad M_{\omega+1}^{(I)} \overset{d}{=} R_M M_\omega^{(I)} \tag{3}$$

where $R_M = E[M_{\omega+1}^{(E)}]/E[M_\omega^{(E)}] = E[M_{\omega+1}^{(I)}]/E[M_\omega^{(I)}]$ is a constant independent of ω and the pseudo-hillslope type. We also found that $M_\omega^{(E)} \overset{d}{\neq} M_\omega^{(I)}$. Tokunaga (2003) investigated the scale independence of the ratio R_M for interior tiles in his analysis of a physical basis of tiling properties of drainage basins.

The distribution for pseudo-hillslope areas and pseudo-magnitudes can be connected by recognizing that the total area for exterior and interior pseudo-hillslopes with magnitude $M_\omega^{(E)}$ and $M_\omega^{(I)}$, respectively, can be written as

$$A_\omega^{(E)} = \sum_{j=1}^{M_\omega^{(E)}} a_j^{(E)} + \sum_{j=1}^{M_\omega^{(E)}-1} a_j^{(I)} \tag{4}$$

$$A_\omega^{(I)} = \sum_{j=1}^{M_\omega^{(I)}} a_j^{(E)} + \sum_{j=1}^{M_\omega^{(I)}+1} a_j^{(I)} \tag{5}$$

where $a_j^{(I)}$ and $a_j^{(E)}$ are interior and exterior hillslope areas, respectively. We can multiply and divide the sums by the total number of terms in each one of them to obtain

$$A_\omega^{(E)} = \frac{\sum_{j=1}^{M_\omega^{(E)}} a_j^{(E)}}{M_\omega^{(E)}} M_\omega^{(E)} + \frac{\sum_{j=1}^{M_\omega^{(E)}-1} a_j^{(I)}}{M_\omega^{(E)}-1}\left(M_\omega^{(E)}-1\right) \tag{6}$$

$$A_\omega^{(I)} = \frac{\sum_{j=1}^{M_\omega^{(I)}} a_j^{(E)}}{M_\omega^{(I)}} M_\omega^{(I)} + \frac{\sum_{j=1}^{M_\omega^{(I)}+1} a_j^{(I)}}{M_\omega^{(I)}+1}\left(M_\omega^{(I)}+1\right) \tag{7}$$

The asymptotic behavior of these sums as ω becomes large can be derived from well-established results in the literature. First, Veitzer and Gupta (2000) investigated the asymptotic behavior of $M_\omega^{(E)}$ for RSNs as $\omega \to \infty$ and demonstrated that

$$\frac{M_\omega^{(E)}}{R_M^{\omega-1}} \to W_M^{(E)} \tag{8}$$

with probability one.[2] Here, $W_M^{(E)}$ is a random variable independent of ω. Troutman (2005) showed that the convergence with probability one also holds for $M_\omega^{(I)}$. Next, the law of large number guarantees, under very general conditions for the random variable $a_j^{(E)}$ and $a_j^{(I)}$, that as $M_\omega^{(E)}$ and $M_\omega^{(I)}$ become large that

$$\lim_{\omega\to\infty} \frac{\sum_{j=1}^{M_\omega^{(E)}} a_j^{(E)}}{M_\omega^{(E)}} = \mu_a^{(E)} \quad \text{and} \quad \lim_{\omega\to\infty} \frac{\sum_{j=1}^{M_\omega^{(E)}-1} a_j^{(I)}}{M_\omega^{(E)}-1} = \mu_a^{(I)} \tag{9}$$

[2] This term indicates the type of convergence of the probability distribution of the random variable. For a technical definition of the term see Ross (2010).

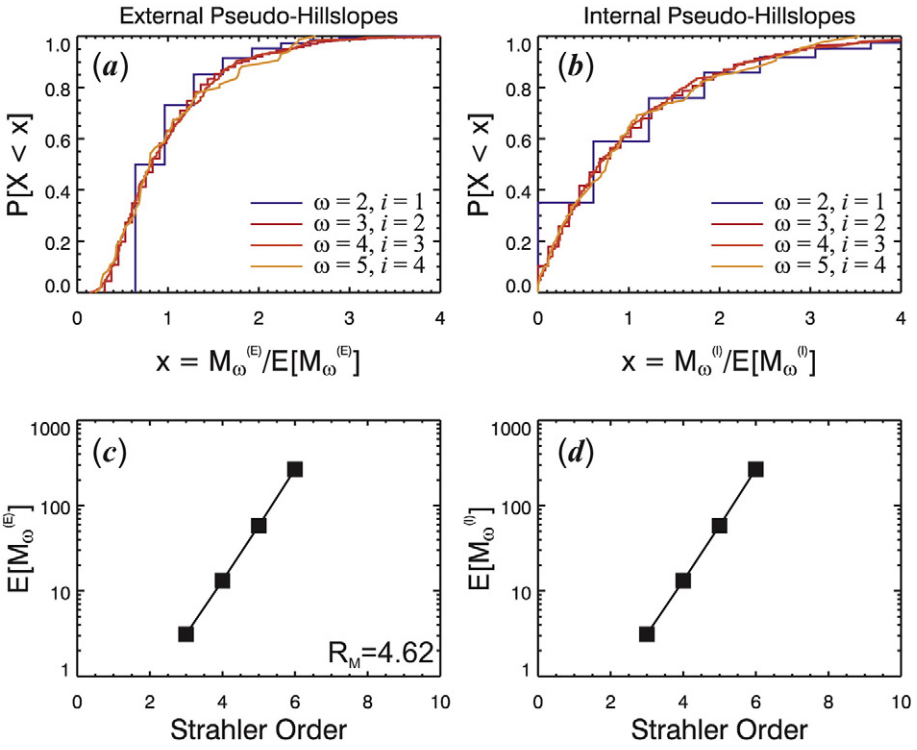

Fig. 8. Extended Generalized Horton laws analysis of pseudo-magnitudes for the Kentucky River basin in northern Kentucky.

$$\lim_{\omega\to\infty}\frac{\sum_{j=1}^{M_\omega^{(I)}} a_j^{(E)}}{M_\omega^{(I)}}=\mu_a^{(E)} \quad \text{and} \quad \lim_{\omega\to\infty}\frac{\sum_{j=1}^{M_\omega^{(I)}+1} a_j^{(I)}}{M_\omega^{(I)}+1}=\mu_a^{(I)} \tag{10}$$

with probability one. Combining these results, it follows that

$$\frac{A_\omega^{(E)}}{\left(\mu_a^{(E)}+\mu_a^{(I)}\right)R_M^{\omega-1}}\to W_M^{(E)} \quad \text{and} \quad \frac{A_\omega^{(I)}}{\left(\mu_a^{(E)}+\mu_a^{(I)}\right)R_M^{\omega-1}}\to W_M^{(I)} \tag{11}$$

with probability one.

These results lead to the equalities

$$\frac{A_\omega^{(E)}}{\left(\mu_a^{(E)}+\mu_a^{(I)}\right)R_M^{\omega-1}}\overset{d}{=}\frac{M_\omega^{(E)}}{R_M^{\omega-1}} \quad \text{and} \quad \frac{A_\omega^{(I)}}{\left(\mu_a^{(E)}+\mu_a^{(I)}\right)R_M^{\omega-1}}\overset{d}{=}\frac{M_\omega^{(I)}}{R_M^{\omega-1}} \tag{12}$$

when ω is large. If the hillslope areas are statistically independent of network branching, from Eqs. (4) and (5) we can show that $E[A_\omega^{(E)}]\sim(\mu_a^{(E)}+\mu_a^{(I)})E[M_\omega^{(E)}]$ and $E[A_\omega^{(I)}]\sim(\mu_a^{(E)}+\mu_a^{(I)})E[M_\omega^{(I)}]$, where ~ indicates asymptotic equivalence for large ω. Thus, we have

$$\frac{A_\omega^{(E)}}{E\left[A_\omega^{(E)}\right]}\overset{d}{=}\frac{M_\omega^{(E)}}{E\left[M_\omega^{(E)}\right]} \quad \text{and} \quad \frac{A_\omega^{(I)}}{E\left[A_\omega^{(I)}\right]}\overset{d}{=}\frac{M_\omega^{(I)}}{E\left[M_\omega^{(I)}\right]} \tag{13}$$

for large ω.

We test this conclusion for our two basins using the tessellations corresponding to orders $\omega=3,4,$and 5. We performed Kolmogorov–Smirnov tests to confirm the hypothesis of distributional equality in each case, and we plotted quantile–quantile (QQ) plots (NIST/SEMATECH, 2006) in Figs. 9 and 10.

The scaling laws presented here are a direct consequence of the self-similar structure of the river network captured by the RSN model (Troutman, 2005). Mantilla et al. (2010) tested the self-similarity assumption for 30 basins and found that the hypotheses of self-similarity hold for 26 of them. It implies that that set of basins obey scaling of interior pseudo-hillslopes. Therefore, the results presented here are not limited to the two test basins that we have selected. Dataset for the 30 basins used by (Mantilla et al., 2010) along with open source software to calculate these properties is provided at http://www.iihr.uiowa.edu/~ricardo/cuencas/cuencas-download.htm.

In the following section we describe two embedding algorithms and use the extended Horton scaling laws to test their ability to replicate these geomorphic features observed in real landscapes.

4. Embedding algorithms

The main goal of this section is to present two algorithms that encode two possible embedding strategies. The first one is the top-down strategy, in which the landscape is partitioned simultaneously with the river network generation process. This method was first illustrated by Veitzer (1999) and it is presented in this paper mainly for completeness. Second, the bottom-up strategy is described. We present the latter methodology in three subsections, in which we provide (1) a motivation for the development of the algorithm, (2) the technical description of the algorithm and (3) some applications of the algorithm.

4.1. The top-down embedding (TDE) algorithm

Veitzer (1999) proposed an algorithm to embed RSNs in two-dimensional regions based on the iterative fracturing of the region. His tiling algorithm begins with an initial region bounded by a four-sided polygon and then follows the recursive replacement process used to construct RSNs to subdivide this initial region. For the first step, if the generator defining the iteration-1 replacement has k links ($k=2m+1$), where m is the number of interior nodes (see Fig. 2a), then the initial region is divided into k subregions, each itself bounded by a four-sided polygon. Given the shape of the initial polygon and number of subregions k, the fracturing is done using the deterministic rule described by Veitzer (1999). This process is then repeated in an iterative fashion using randomly sampled generators,

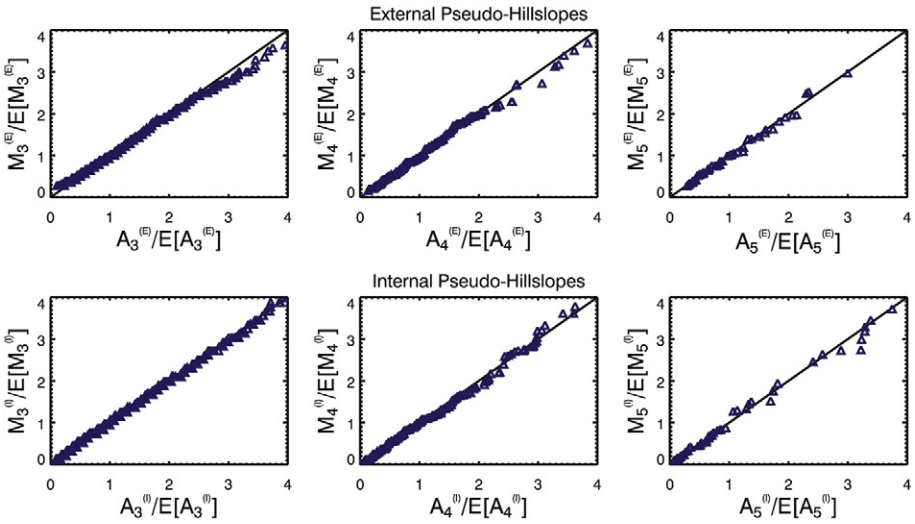

Fig. 9. Quntile–quantile plots comparing pseudo-magnitudes and pseudo-hillslope areas distributions for pruning levels 2, 3 and 4 ($\omega = 3$, 4, and 5) in the Walnut Creek Basin in Kansas.

with the subdivision at each step depending on the number of nodes in the generator being embedded and with the fraction of area associated with each link of the generator prescribed by the deterministic rule. We refer to this algorithm as a top-down embedding (TDE) algorithm because areas at large scales are determined first without regard to the subsequent branching that takes place at smaller scales.

To better understand the algorithm, consider the instance of RSN in Fig. 11, where exterior links are replaced by E1 generators and interior links are replaced by I3 generators with probability one[3] (see Fig. 2 for definitions of generators). In Fig. 11 the replacement process starts with one link; the link is replaced by an E1 generator. In the next step, exterior links are replaced by E1 generators, while interior links are replaced by I3 generators. After one more iteration, the total number of links in the tree is 63. Following the same rule for sampled generators, we apply the TDE algorithm to the region in Fig. 12a. The initial four-sided region is divided into 3 four-sided subregions (Veitzer, 1999). Then exterior subregions are divided into 3 subsubregions and interior subregions are divided into 7 subsubregions. After two more iterations, the initial region is partitioned into 63 tiles (Fig. 12d).

Veitzer (1999) discusses properties of the resulting statistical distribution of tile areas in the final tessellation using this algorithm. He reports that, in most of the cases examined, the tessellation exhibits a 'divergence' between the largest and the smallest value of tile area that is not empirically observed in hillslope areas in natural river basins (see Mantilla and Gupta (2005) for definition of hillslope). This feature can be interpreted by relating the tiling procedure to a multifractal cascade formalism (Holley and Waymire, 1992; Gupta and Waymire, 1993) under which mass accumulation shows such divergence.

Note that the way in which subregion areas are allocated at each step of a TDE algorithm is the fundamental ingredient of the algorithm. This process is governed in the algorithm of Veitzer (1999) by the deterministic rule used to fracture four-sided polygons. The areas of subregions produced by such fracturing are not in general equal; in fact, with this algorithm it is not possible to explicitly control sub region areas at each step. To examine this issue more carefully, we performed an experiment with the RSN model in which descendants of a link following a replacement were assigned exactly the same proportion of 'area'. The networks were not embedded spatially, but we could still examine the resulting pseudo-hillslope area distribution at each level of the iteration. The number of interior nodes (see Fig. 2) for all generators was taken to have a geometric distribution given by $P(K_i = k_i) = p_i(1-p_i)^{k_i}$, $k_i \geq 0$ for interior generators and $P(K_e = k_e) = p_e(1-p_e)^{k_e-1}$, $k_e \geq 1$ for exterior generators, with parameter $p_I = 0.42$ and $p_E = 0.49$. We define a random variable K_i as the number of interior nodes in interior generators and the random variable K_e as the number of interior nodes in exterior generators (see Fig. 2 for node types). Note that for exterior generators, the condition $k_e \geq 1$ follows from the type of generators that we are using. Thus the random variables K_i and $K_e - 1$ are taken to have a geometric probability distribution with parameters p_i and p_e respectively. The geometric distribution was found in the study by Mantilla et al. (2010) to be appropriate for modeling actual river networks. The distributions of $A_\omega^{(E)}/E[A_\omega^{(E)}]$ and $A_\omega^{(I)}/E[A_\omega^{(I)}]$ stabilized after 10 iterations, and in Fig. 13 we compare these stable distributions to those of the scaled pseudo-magnitudes $M_\omega^{(E)}/E[M_\omega^{(E)}]$ and $M_\omega^{(I)}/E[M_\omega^{(I)}]$ for the RSN model. The distributions differ for both exterior and interior pseudo-hillslopes, indicating that assignment of exactly the same proportion of area to subregions at each step of the RSN construction does not yield pseudo-hillslope area distributions that agree with the corresponding pseudo-magnitude distributions. Such agreement holds in real basins, as previously shown.

4.2. The bottom-up embedding algorithm (BUE)

4.2.1. Motivation for the development of BUE algorithm

In this section we introduce a new approach to embedding trees called bottom-up embedding (BUE) algorithms. The 'bottom-up' label refers to the fact that such algorithms factor in the branching that takes place at small scales to define areas at larger scales. To see why this is important, we first consider a result presented by Troutman (2005). He showed that in the RSN model the asymptotic number of descendants of interior links is, on average, different from the number of descendants of exterior links, and the ratio between these average numbers can be computed exactly given the distributions of number of nodes in generators. For example, in the experiment in the previous paragraph, we see that exterior links will on average give rise to 2.29 times more descendants than interior generators. This suggests that, in any spatial embedding of RSNs obtained with $p_I = 0.42$ and $p_E = 0.49$, exterior tiles should be given 2.29 times more area than interior tiles in order to try to maintain nearly constant drainage density, in contrast to the equal area assignments made in TDE. The experiment illustrated in the previous section was repeated with this correction (results not shown here), but

[3] Notice that assigning replacement generators with probability one gives rise to SSTs.

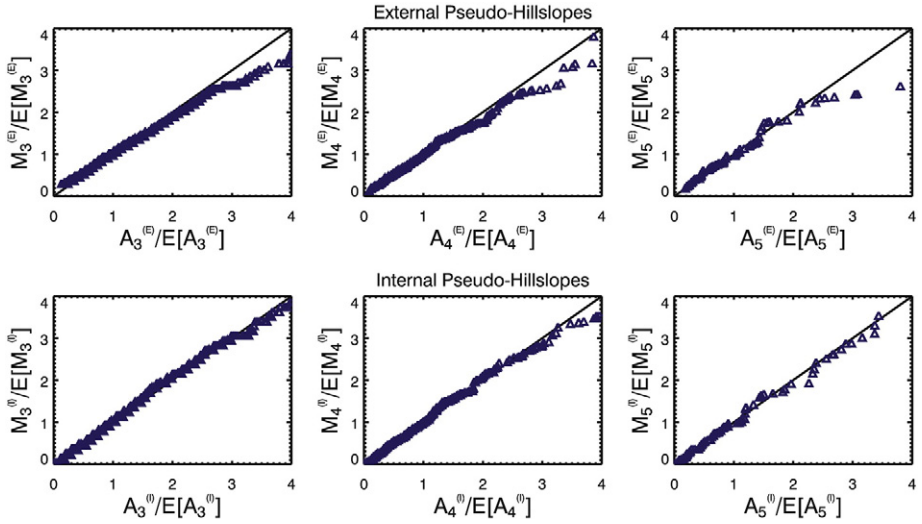

Fig. 10. Quntile–quantile plots comparing pseudo-magnitudes and pseudo-hillslope areas distributions for pruning levels 2, 3 and 4 ($\omega = 3$, 4, and 5) in the Kentucky River Basin in Kentucky.

again we observed a discrepancy between the pseudo-magnitude and pseudo-hillslope area distributions (see details in Mantilla (2007)). The problem is that allocation of area based solely on *average* number of descendants is not sufficient to ensure correct area scaling.

We now carry the idea of unequal subregion area allocation one step further to incorporate even more information on small-scale branching at large scales. Suppose a network of given order generated by the RSN model is to be embedded. If the entire topological network is generated first (down to a predetermined level) and hillslope areas are assigned to each link in the resulting network, then pseudo-hillslope areas for each level i can be calculated exactly by simply aggregating the appropriate elementary hillslope areas. Embedding can still be done in the same iterative fashion as before, but at each step the precise area that should be allocated to each generator link at each scale is known beforehand. The process is thereby guaranteed to produce a tree with pseudo-magnitudes proportional to pseudo-hillslope areas at all scales, so upstream areas will inherit scaling properties of magnitudes. This conditioning at each iteration on the entire tree and known elementary hillslope areas is the essence of the BUE algorithm we propose in this paper.

The two key inputs to the BUE algorithm are the river network topology and the hillslope areas. If the RSN model generates the river network, exterior pseudo-magnitudes will exhibit the scaling shown in Eq. (8), and interior pseudo-magnitudes will scale similarly. A sufficient condition for pseudo-hillslope areas to show the same scaling as magnitudes is that Eqs. (9) and (10) (law of large numbers) hold for the hillslope areas, and whether these equations hold depends on assumptions made on hillslope areas. The simplest case for which they hold is when the hillslope areas $a_j^{(I)}$ and $a_j^{(E)}$ are constant. A more realistic case is that for which each is a set of independent and identically distributed (i.i.d.) random variables (which are also independent of the network). We know further that the law of large numbers will also hold in some cases when correlation is present in the summands, as long as the correlation is weak.

One obvious source of correlation among hillslope areas that may be introduced in embedding networks with the BUE algorithm is a consequence of the finite space in which the network is being embedded. Assume that it is desired to embed the network in a given finite region, and that hillslope areas are simulated using an i.i.d. model. Because the sum of all hillslope areas must equal the total network embedding area, each hillslope area must be scaled by the sum of hillslope areas in such a way that this equality holds. Doing this induces correlation among the hillslope areas, however it has been demonstrated that the degree of correlation in such cases is small (see Pyke, 1965).

We performed computer simulations for which the network was obtained by the RSN model and hillslope areas are taken to be (1) constant, (2) i.i.d. exponentially distributed random variables, and (3) correlated (i.i.d. exponential hillslope areas scaled by the sum). Fig. 14 shows the scaled pseudo-hillslope area distributions for the first five iteration steps of scenario (2). We see that there is a rapid convergence to a scale-independent distribution, as it was also the case for scenarios (1) and (3). We also confirmed that the scaled pseudo-hillslope area distribution is in all three cases, after eight iterations, identical to the scaled pseudo-magnitude distribution. We conclude that in these three cases the effect of hillslope area variation or correlation is overwhelmed by the effect of the aggregation and that the randomness in the system is dominated by the network branching structure.

Finally, we compare the distribution of areas found in data with the stable distribution under BUE. In Fig. 15 we plotted the Q–Q diagram for the distribution of $A_\omega^{(E)}/E[A_\omega^{(E)}]$ and $A_\omega^{(I)}/E[A_\omega^{(I)}]$ derived from data and from the stable BUE for orders $\omega = 3, 4,$ and 5. The remarkable fit found indicates that the branching structure of the network determines the statistical nature of the pseudo-hillslope areas.

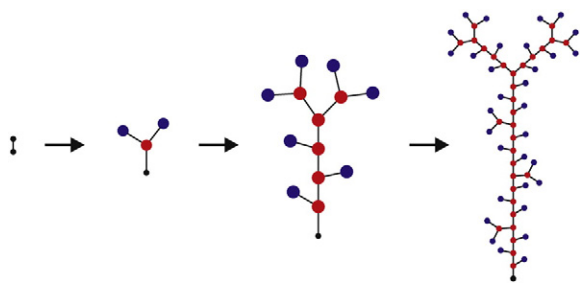

Fig. 11. Sample RSN using E1 generators for exterior links with probability one and I3 generators for interior links with probability one.

4.2.2. Description of the BUE algorithm

The essence of the BUE algorithm is a recursive strategy for dividing the region using the information from the recovered generators that make up the network (Troutman, 2005; Mantilla, 2007).

To simplify the description of the recursive algorithm, we shall give it in two parts. The first portion is the embedding of a simple generator in a polygon, and the second describes the embedding of a complex tree (decomposed into generators).

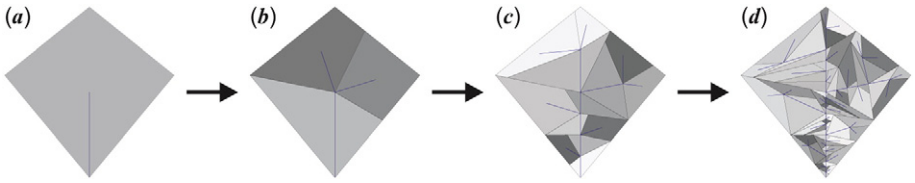

Fig. 12. Tiling of a two-dimensional region according to the TDE algorithm.

The steps for embedding a simple generator are easy to follow and they are schematically described in Fig. 16 using the case of an E2 generator. Let this algorithm be called the simple tree embedding (STE) algorithm. The steps of the process are:

1. Assign a value of area to every link in the generator (here the total area of the links has to equal the area of the polygon).
2. Determine the bottom region by scanning upwards from the lowest polygon vertex until the area equals that of the bottom link. We define the line that is used in the scanning process as the *scanning line*.
3. Assign the location of the river by connecting the polygon vertex to the middle of the final *scanning line*. We call the latter location a *connecting node*.
4. Find an intermediate region for the two upstream links with area equal to the sum of these branches (the two branches are one interior and one exterior, or two exterior links). The scanning line moves upward from the last location determined in the previous step.
5. Divide the sub region into two tiles, with areas assigned to each branch. The scanning process is done with a *breaking line* that connects the location of the previously determined river and the intermediate region border.
6. Assign the locations of the two rivers. One is connected to the border of the intermediate region and the other one is not. The new location of the intersection establishes a new connecting node.
7. Finally repeat steps (4), (5) and (6) until the top of the polygon is reached. At this point the location of the two final exterior links is determined.

Here, emphasis needs to be made on the importance of determining the location of the upper link node on the scanning line. Notice that this point determines the initial node of the *breaking line*, used in the algorithm. Also notice that the final step in the embedding of a simple generator ended with two exterior links. For generality, consider that if one of the two final links were treated as interior it would be a matter of connecting such link to a point in the polygon border generating a new connecting node location. This consideration is essential to understand the recursive algorithm that follows.

Now that the embedding of the simple tree has been explained we can move on to the description of the recursive embedding process. The steps of the process are the following:

1. Determine (*i*) the sequence of generators required to construct the topology to be embedded and (*ii*) the number of iterations Ω needed to construct the tree. The decomposition method has been carefully explained in Mantilla (2007) in the context of RSNs.
2. Assign a value of area to every link in the tree.
3. Proceed to break the region enclosed by a convex polygon into as many pieces as the iteration-1 generator dictates. Notice that the iteration-1 generator corresponds to one of the basic exterior

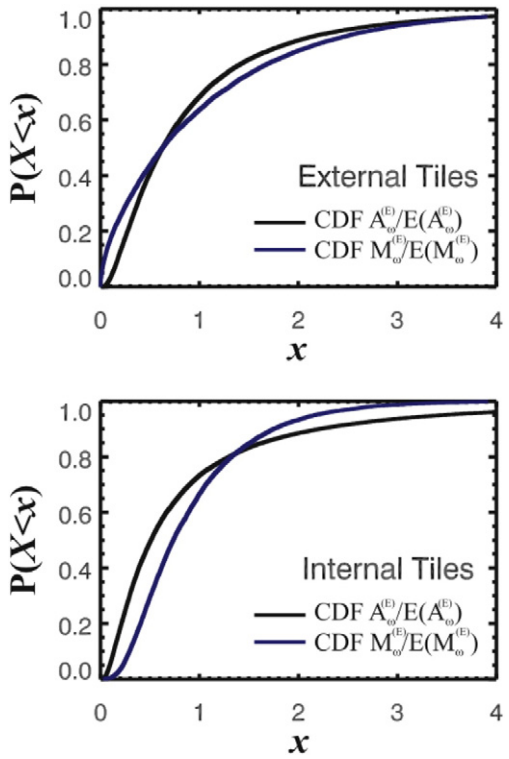

Fig. 13. Stable distribution of tile areas and magnitudes divided by their means.

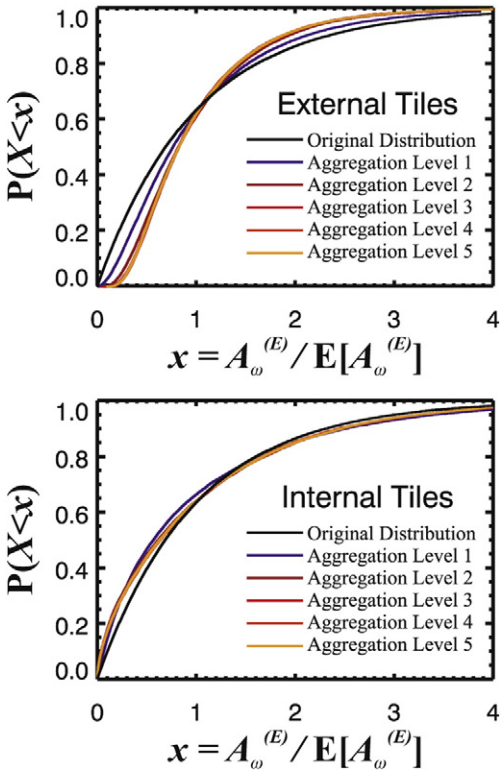

Fig. 14. Cumulative distribution functions of $A_\omega^{(E)}/E[A_\omega^{(E)}]$ and $A_\omega^{(I)}/E[A_\omega^{(I)}]$ in five consecutive steps of the aggregation process.

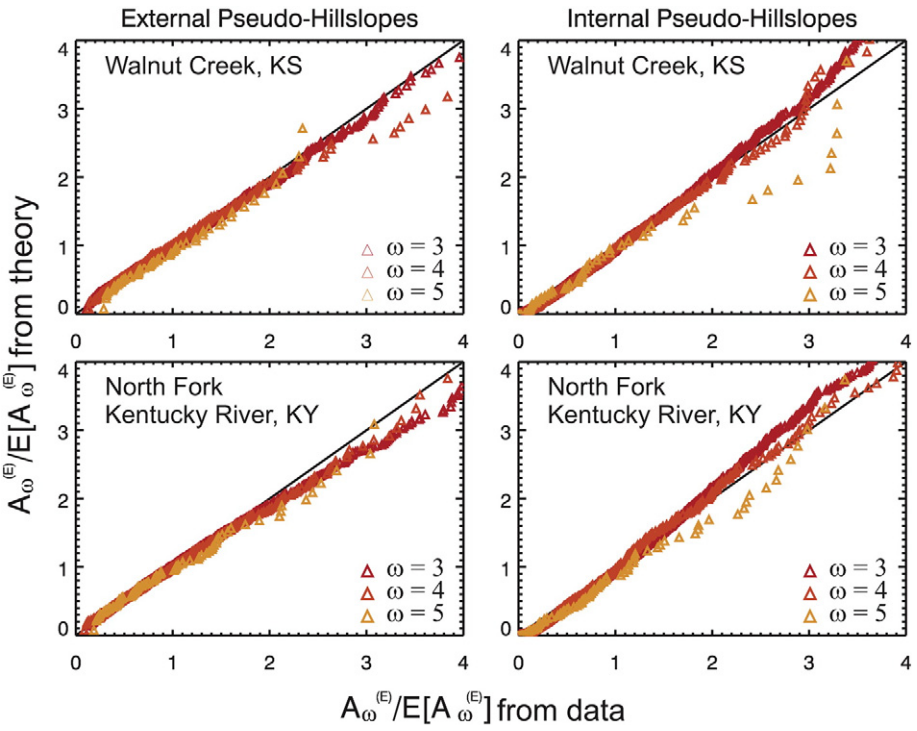

Fig. 15. Quantile–quantile plots of $A_\omega^{(E)}/E[A_\omega^{(E)}]$ and $A_\omega^{(I)}/E[A_\omega^{(I)}]$ derived from data in the Walnut Creek basin in Kansas, and the North Fork Kentucky River vs. the BUE stable distribution for orders $\omega = 3$, 4 and 5.

generator types in Fig. 2a; thus, we can apply the STE algorithm to this region. Here attention should be given to the fact that the total area of the 'generator links' is determined by the sum of the area of their *progeny*. We define the progeny of link *e* as all the links that spawn from the replacement process that starts with link *e*.

4. As indicated by the algorithm for simple generators, the first step is to determine the bottom region.
   (a) Determine the iteration-2 generator that spawns from the link being embedded. In a recursive fashion apply steps (4) and (5) to the current polygon until the iteration-Ω generator has been reached. At this point apply the algorithm for simple generators described previously.
   (b) Now step outward in a recursive fashion until the bottom region has been fully distributed amongst the links of the spawning link.

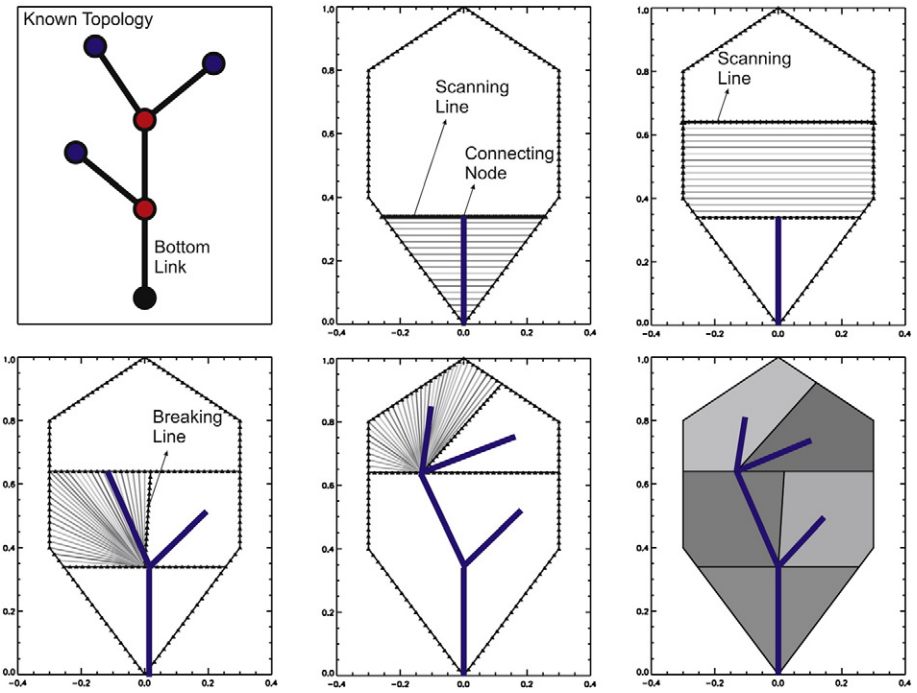

Fig. 16. Steps for embedding the topology of an E2 generator.

5. As indicated by the STE algorithm, the second step is to determine the intermediate region.
   (a) Determine the iteration-2 generator that spawns from the link being embedded. In a recursive fashion apply steps (4) and (5) to the current polygon until the iteration-Ω generator has been reached. At this point apply the STE algorithm.
   (b) Now step outward in a recursive fashion until the intermediate region has been fully distributed amongst the links of the spawning tree.
6. Finally determine the top region and apply steps (3) and (4) in a recursive fashion.

The recursive nature of the algorithm is necessary because, although the total area of each subregion is known, the location through which the river will flow out of the tile is unknown. The process can be better illustrated by applying the algorithm to topologies with increasing complexity. Examples are presented in the following section.

4.2.3. Applications of the BUE algorithm

In this section we present some applications of the algorithm to SSTs and to RSNs. The topologies and initial shape were selected for simplicity and to illustrate how different topologies embed into the same shape. Some produce realistic tile shapes and others do not. The issue of the relation between shape and topology is an area of further research that is not addressed in this paper.

Self similar trees can be generated by sampling a single interior generator type to replace interior links and a single exterior generator type to replace exterior links during the RSN generation process. The tree in Fig. 11, generated by replacing exterior links with E1 generators and interior links with I3 generators, is an example of one such tree. We introduce the notation Ek_1Ik_2 to characterize these SSTs. Here, k_1 and k_2 are integers representing the generator type that is used to replace exterior and interior links, respectively. Thus, the tree in Fig. 11 is denoted E1I3. Fig. 17 shows the tiled region for SSTs E1I1, E1I3, E2I1, and E2I2. In these four cases we have chosen to assign tile area $a_j^{(E)} = a_j^{(I)} = A_\Omega/(2M_\Omega + 1)$, where A_Ω is the total region area and M_Ω is the BRT magnitude.

To illustrate the generality of the algorithm, we have created RSNs, with random generators following a geometric distribution. We selected parameters $p_E = 0.49$ for exterior generators and $p_E = 0.42$ for interior generators. Fig. 18 shows the resulting tiling for these trees after four generations. Once again we assign tile area $a_j^{(E)} = a_j^{(I)} = A_\Omega/(2M_\Omega + 1)$.

5. Artificial three-dimensional landscapes

In addition to creating two-dimensional tiled regions, the BUE can be extended to create three-dimensional surfaces with drainage properties that fully correspond to the intended network. Fig. 19 shows the landscape generated for the embedded E1I1 network. Projecting points of the embedded network, and the corresponding tessellation, into a two-dimensional matrix, generates these artificial landscapes. The points to project correspond to the location of the network edges and the tile borders.

We ensure that the channel network will flow in the correct direction by assigning an elevation value to the network edges proportional to the topologic distance to the outlet. Next, we assign the value of two times the maximum distance to the outlet along the network to the locations in the matrix that correspond to the tile borders. Finally, we use these reference points to create a triangulation (Lee and Schachter, 1980) that is used to linearly interpolate values for the rest of the positions in the matrix. This step is necessary because the flow direction is only known for those pixels along the streams. The linear interpolation provides elevations at hillslope pixels in such a way that the maximum gradient is in the direction of the intended link. A similar algorithm was developed by Sun et al. (1994) in the context of optimal channel networks, but their algorithm relied on a direction matrix prescribing a drainage direction to every cell of the lattice.

Note that the algorithm can be easily modified to include more realistic elevation changes along the network in order to obtain more realistic slopes throughout the watershed. Landscapes obtained in this manner would make ideal initial conditions for landscape evolution models (e.g. Birnir et al., 2001; Birnir et al., 2007), as they would provide a more predictable outcome for the drainage network topology.

6. Conclusions

We presented an extension of generalized Horton laws of landscape composition that reveals new and interesting scaling features of real river basins. We called this framework 'extended generalized Horton laws'. The extension of Horton laws is inspired by recent theoretical results by Tokunaga (2003) regarding scaling properties of internal sub basins of Tokunaga trees and other deterministic networks such as the Peano network or the Mandelbrot–Viscek tree, and by results in Troutman (2005) that demonstrated similar scaling properties for RSN topologies. The link between the empirical results presented in this paper and theoretical results on RSNs and self-similar topologies provide a context for these new Horton laws, in which the single principle of statistical self-similarity of the structure of the network explains several scaling laws instead of viewing them as independent of each other. Understanding the connection between the empirical laws of network composition in the context of self-similarity provides new techniques for the estimation of the parameter values (i.e. R_A, R_M, R_L, etc.) that can address estimation issues highlighted by other authors (e.g. Puente and Castillo (1996); Moussa (2009)).

The extended generalized Horton laws are used to evaluate two embedding algorithms that we call Top-Down and Bottom-Up embedding, TDE and BUE, respectively. We demonstrated that the TDE approach is inappropriate to create tessellations of a region that correspond to those found in real landscapes because the areas of the tiles in TDE are highly correlated. It leads to a violation of equality in distribution of rescaled areas and network magnitudes across scales, a property which is found to hold in data.

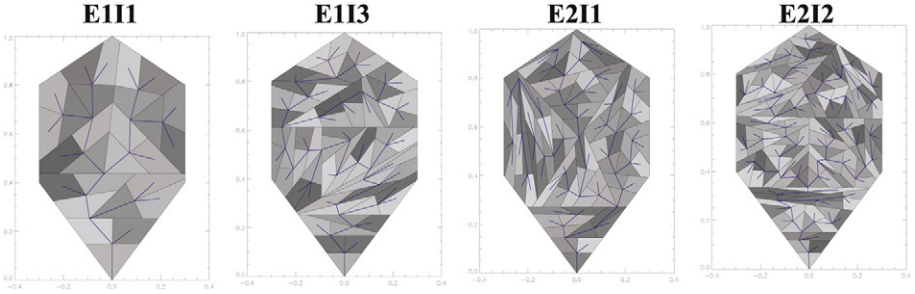

Fig. 17. Bottom up embedding algorithm applied to four self similar trees.

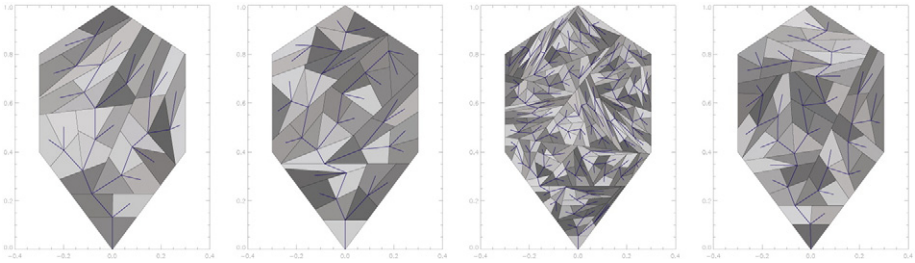

Fig. 18. Bottom up embedding algorithm applied to four order-4 RSNs.

BUE is a new embedding method presented and tested here. The algorithm design allows branching that takes place at small scales to constrain areas at larger scales so that all hillslope areas are assigned in advance of the embedding process. If the topologic tree to be embedded obeys the Extended Generalized Horton Laws for magnitude, then the BUE will always produce an embedded network obeying distributional equality of rescaled magnitude and area.

We used the tiled region to create three-dimensional landscapes with drainage properties established a priori. We argued that these landscapes could be used as the initial condition for landscape evolution models. The landscapes can also be treated as real DEMs to be used in rainfall–runoff simulations.

7. Future work

It is important to note that the extension of Horton laws to Areas and Magnitudes presented in this paper points to the need to test further properties such as river length, topological diameter, slopes, and other geometric and topologic quantities. Testing these scaling laws and developing algorithms that capture their correct scaling features is an important area of future research. In particular we have been experimenting with embedding algorithms that preserve Hack's law (Hack, 1957), however these algorithms have proven far more complex than those introduced in here.

The process of embedding BRTs in two-dimensional regions establishes the bridge between topologic network structure and spatial variability of runoff generation processes. In an upcoming paper, we investigate the interaction between space–time rainfall variability and network topology using the DEMs generated by the BUE. Additional lines of research involve improving the algorithm to obtain hillslope shapes that are more realistic and that impose the additional constraint of preserving Hack's law. The results of this paper are opening the door to an exciting research area rather than the solution to this complex and interesting problem.

Another important area of research is the study of relations between basin shape and network topology. The initial results obtained with the BUE algorithm indicate that when arbitrary network topologies are embedded in arbitrary basin shapes the resulting tiling produces unrealistic shapes because natural river basin shapes influence their network topologies. The results obtained by Mantilla et al. (2010) have shown that RSN generators can be estimated for natural river network. This procedure can be used to understand how basin shapes affect network topologies.

Acknowledgments

We thank Oscar J. Mesa for the very helpful discussion and insightful comments. We also thank Thomas Over and Roland Viger for thorough reviews that led to an improved manuscript. This research was partially supported by a grant from the National Science Foundation to the University of Colorado, and by the Iowa Flood Center at The University of Iowa. This support is gratefully acknowledged.

References

Birnir, B., Smith, T.R., Merchant, G.E., 2001. The scaling of fluvial landscapes. Computers and Geosciences 27, 1189–1216.
Birnir, B., Hernandez, J., Smith, T.R., 2007. The stochastic theory of fluvial land surfaces. Journal of Nonlinear Science 17 (1), 13–57.
Dodds, P.S., Rothman, D.H., 2000. Scaling, universality, and geomorphology. Annual Review of Earth and Planetary Sciences 28 (1), 571–610.
Gupta, V.K., Waymire, E.C., 1993. A statistical analysis of mesoscale rainfall as a random cascade. Journal of Applied Meteorology 32 (2), 251–267.
Gupta, V.K., Castro, S.L., Over, T.M., 1996. On scaling exponents of spatial peak flows from rainfall and river network geometry. Journal of Hydrology 187, 81–104.
Gupta, V.K., Mantilla, R., Troutman, B.M., Dawdy, D., Krajewski, W.F., 2010. Generalizing a nonlinear geophysical flood theory to medium-sized river networks. Geophysical Research Letters 37, L11402.
Hack, J.T., 1957. Studies of longitudinal profiles in Virginia and Maryland. USGS Professional Paper 294–B, United States Geological Survey.
Holley, R., Waymire, E., 1992. Multifractal dimensions and scaling exponents for strongly bounded random cascades. Annals of Applied Probability 2 (4), 819–845.
Horton, R.E., 1945. Erosional development of streams and their drainage basins; hydrophysical approach to quantitative morphology. Geological Society of America Bulletin 56, 275–370.
Lee, D.T., Schachter, B.J., 1980. Two algorithms for constructing a delaunay triangulation. International Journal of Parallel Programming 9 (3), 219–242.
Leopold, L.B., Langbein, W.B., 1962. The concept of entropy in landscape evolution. Professional Paper 500-A. U.S. Geological Survey, Washington D C.
Mantilla, R., 2007. Physical basis of statistical scaling in peak flows and stream flow hydrographs for topologic and spatially embedded random self-similar channel

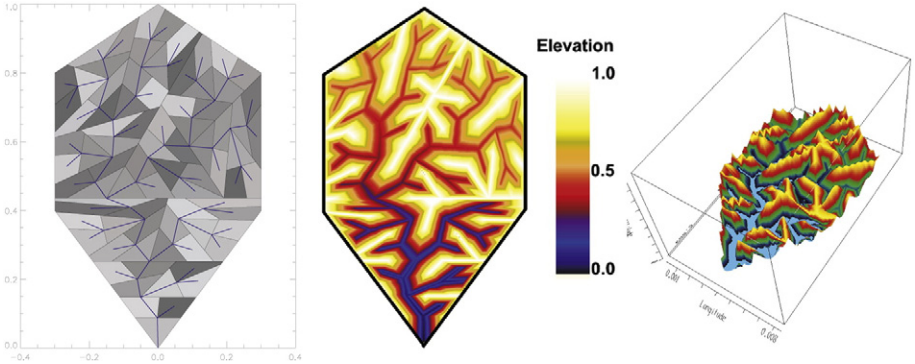

Fig. 19. An example of a three-dimensional landscape obtained from the tessellation generated by the BUE algorithm.

networks. Ph.D. thesis, Department of Civil and Environmental Engineering. University of Colorado, Boulder, CO.
Mantilla, R., Gupta, V.K., 2005. A GIS framework to investigate the process basis for scaling statistics on river networks. Geoscience and Remote Sensing Letters, IEEE 2 (4), 404–408.
Mantilla, R., Troutman, B.M., Gupta, V.K., 2010. Testing statistical self-similarity in the topology of river networks. Journal of Geophysical Research 115, F03038.
Maritan, A., Colaiori, F., Flammini, A., Cieplak, M., Banavar, J.R., 1996. Universality classes of optimal channel networks. Science 272 (5264), 984–986.
McConnell, M., Gupta, V.K., 2008. A proof of the Horton law of stream numbers for the Tokunaga model of river networks. Fractals-Complex Geometry Patterns and Scaling in Nature and Society 16 (3), 227–233.
Meakin, P., Feder, J., Jøssang, T., 1991. Simple statistical models of river networks. Physica A 176, 409–429.
Menabde, M., Sivapalan, M., 2001. Linking space–time variability of rainfall and runoff fields on a river network: a dynamic approach. Advances in Water Resources 24, 1001–1014.
Mesa, O.J., Gupta, V.K., 1987. On the main channel length–area relationship for channel networks. Water Resources Research 23 (11), 2119–2122.
Molnar, P., 2005. On geometrical scaling of cayley trees and river networks. Journal of Hydrology 322 (1–4), 199–210.
Moussa, R., 2009. Definition of new equivalent indices of Horton–Strahler ratios for the derivation of the Geomorphological Instantaneous Unit Hydrograph. Water Resources Research 45 (9).
NIST/SEMATECH, 2006. e-Handbook of Statistical Methods. NISThttp://www.itl.nist.gov/div898/handbook/.
Peckham, S., 1995. New results for self-similar trees with applications to river networks. Water Resources Research 31 (4), 1023–1029.
Peckham, S., Gupta, V.K., 1999. A reformulation of Horton's laws for large river networks in terms of statistical self-similarity. Water Resources Research 35 (9), 2763–2777.
Puente, C.E., Castillo, P.A., 1996. On the fractal structure of networks and dividers within a watershed. Journal of Hydrology 187 (1–2), 173–181.
Pyke, R., 1965. Spacings. Journal of the Royal Statistical Society. Series B 27 (3), 395–449.
Rigon, R., Rodríguez-Iturbe, I., Ijjasz-Vasquez, E., 1993. Optimal channel networks: a framework for the study of river basin morphology. Water Resources Research 29 (6), 1635–1646.
Rinaldo, A., Banavar, J.R., Maritan, A., 2006. Trees, networks, and hydrology. Water Resources Research 42, W06D07.
Rodríguez-Iturbe, I., Rinaldo, A., 1997. Fractal River Basins: Chance and Self-organization. Cambridge University Press, New York.
Ross, S., 2010. First Course in Probability. Pearson.
Scheidegger, A.E., 1967. A stochastic model for drainage patterns into an intramontane trench. Bulletin de l'Association Internationale d'Hydrologie Scientifique 12, 15–20.
Schumm, S.A., 1956. Evolution of drainage systems and slopes in badlands at Perth Amboy, New Jersey. Geological Society of America Bulletin 67, 597–646.
Shreve, R., 1966. Statistical law of stream numbers. Journal of Geology 74, 17–37.
Shreve, R., 1967. Infinite topologically random channel networks. Journal of Geology 75, 178–186.
Strahler, A.N., 1957. Quantitative analysis of watershed geomorphology. American Geophysical Union Transactions 8 (6), 913–920.
Sun, T., Meakin, P., Jossang, T., 1994. The topography of optimal drainage basins. Water Resources Research 30, 2599–2611.
Tokunaga, E., 1966. The composition of drainage network in Toyohira river basin and valuation of Horton's first law. Geophysical Bulletin of Hokkaido University 15, 1–19 in Japanese with English summary.
Tokunaga, E., 2003. Concepts and modelling in geomorphology: international perspectives. TERRAPUB, Tokyo, Japan, Ch. Tiling Properties of Drainage Basins and Their Physical Bases, pp. 147–166.
Troutman, B.M., 2005. Scaling of flow distance in random self-similar channel networks. Fractals 13 (4), 265–282.
Troutman, B.M., Karlinger, M.R., 1994. Inference for a generalized Gibbsian distribution on channel networks. Water Resources Research 30 (7), 2325–2338.
Troutman, B., Karlinger, M., 1998. Spatial channel network models in hydrology. In: Barndorff-Nielsen, O.E., Gupta, V.K., Pérez-Abreu, V., Waymire, E. (Eds.), Stochastic Methods in Hydrology: Rain, Landforms and Floods. : Vol. 7 of Advanced Series on Statistical Science and Applied Probability. World Scientific, Singapore, pp. 85–128.
Troutman, B.M., Over, T.M., 2001. River flow mass exponents with fractal channel networks and rainfall. Advances in Water Resources 24, 967–986.
Veitzer, S., 1999. A theoretical framework for understanding river networks: connecting process, geometry and topology across many scales. Ph.D. thesis, Department of Civil and Environmental Engineering. University of Colorado, Boulder.
Veitzer, S., Gupta, V.K., 2000. Random self-similar river networks and derivations of Horton-type relations exhibiting statistical simple scaling. Water Resources Research 36 (4), 1033–1048.
Veitzer, S., Troutman, B., Gupta, V.K., 2003. Power-law tail probabilities of drainage areas in river basins. Physical Review E 68, 016123.